Oximes as Reversible Links in Polymer Chemistry: Dynamic Macromolecular Stars

Journal:	*Polymer Chemistry*
Manuscript ID:	PY-ART-09-2014-001282
Article Type:	Paper
Date Submitted by the Author:	18-Sep-2014

Complete List of Authors:	Mukherjee, Soma; University of Florida, Department of Chemistry Bapat, Abhijeet; University of Florida, Department of Chemistry Hill, Megan; University of Florida, Chemistry; University of Florida, Department of Chemistry Sumerlin, Brent; University of Florida, Department of Chemistry;

Journal Name

RSCPublishing

ARTICLE

Oximes as Reversible Links in Polymer Chemistry: Dynamic Macromolecular Stars

Cite this: DOI: 10.1039/x0xx00000x

Soma Mukherjee, Abhijeet P. Bapat, Megan R. Hill and Brent S. Sumerlin*

Received 00th September 2012,
Accepted 00th September 2012

DOI: 10.1039/x0xx00000x

www.rsc.org/

We demonstrate the formation of oxime-functional macromolecular stars that are able to dissociate and reconstruct themselves upon application of a stimulus. The reversible nature of the oxime bond in the presence of externally added alkoxyamines or carbonyl compounds enables reconfiguration *via* competitive exchange. Reversible addition-fragmentation chain transfer (RAFT) polymerization was utilized to prepare well-defined amphiphilic block copolymers in which a hydrophobic keto-functional block allowed self-assembly into micelles in water. Adding a difunctional alkoxyamine small molecule to these solutions resulted in crosslinking of the micelles to yield macromolecular stars. The reversible nature of the *O*–alkyl oxime linkages was demonstrated *via* competitive exchange with excess of carbonyl compounds or monofunctional alkoxyamine under acidic conditions and at elevated temperatures to result in dissociation of the stars to unimolecular oxime-functional polymer chains.

Introduction

Macromolecules containing readily reversible covalent bonds offer potential as new degradable, responsive, and adaptable materials. A variety of reversible linkages have been used to access such "dynamic-covalent" polymers, with imines and acyl hydrazones having proven particularly promising.[1,2-4] The reversibility of oxime bonds has received less attention, possibly due to their greater stability as compared to imines or hydrazones.[5] However, it is exactly this enhanced stability, especially with respect to hydrolysis, which confers considerable promise on oxime formation for the construction of dynamic-covalent materials that can be triggered to exchange their components only under a specific set of conditions. Eliseev and coworkers have studied the kinetics and mechanism of imine exchange between various small molecule oximes and *O*–alkyl or *O*–aryloxyamines, and suggested the possibility of creating a library of oxime compounds that can shuffle or rearrange functionalities under appropriate conditions.[6] Recently, Yousaf and co-workers exploited the reversibility of oxime linkages to engineer cell surfaces to allow programmed assembly and disassembly to form 3D tissues for applications in stem-cell differentiation and tissue engineering.[7]

Post-polymerization modification of aldehyde- or ketone-containing polymers with alkoxyamines has also received significant attention due to high reaction yields, catalyst-free/mild reaction conditions (ambient temperature, aqueous environment), and benign side-product (water).[5,8] Francis *et al*. utilized oxime formation to prepare thermoresponsive protein-polymer bioconjugates,[9] to incorporate an anti-freeze protein in a polymer coating for devices that function at low temperature without ice-build up,[10] and to construct protein functionalized hydrogels.[11] Maynard *et al*. prepared micropatterned alkoxyamine functionalized polymer films to conjugate an *α*-ketoamide modified protein by employing oxime formation and a photolithography technique,[12] and later demonstrated covalent immobilization of site-selectively modified protein onto a gold surface by microcontact printing and bio-orthogonal click reactions, including oxime ligation.[13] These reports clearly demonstrate the utility of oxime formation for the construction of stable and robust macromolecular materials. However, the potential of oxime containing polymeric materials to be rendered reversible under a specific set of conditions has not been fully considered.

Given its high efficiency and selectivity, oxime formation should be a valuable method to facilitate the synthesis of polymers with complex macromolecular architecture.[8] We have recently reported reversible addition-fragmentation chain transfer (RAFT) polymerization of an alkoxyamine containing monomer and subsequent functionalization of the polymers with small molecule aldehydes and ketones.[14] Theato *et al.* reported controlled polymerization of acetone oxime acrylate and then used *N*-isopropylamine to partially convert the acetone oxime groups in the polymer to yield thermoresponsive poly(*N*-isopropylamine-*co*-acrylamide).[15] An alternative approach would be to include the requisite aldehyde or ketone functionality in the polymer and to functionalize with small molecule alkoxyamines. Aldehyde-containing polymers have been demonstrated to be useful reactive scaffolds, and keto-functional polymers have recently begun receiving similar interests.[8,16,17,18,19] Potentially, the greater stability of ketones toward oxidation in aqueous media as compared to aldehydes renders them ideal for biological applications.[16] For this reason, we have chosen to focus here on well-defined ketone-containing polymers as reactive scaffolds for functionalization with low molecular weight *O*–alkoxyamines. Control over molecular

weight and dispersity of the reactive functional polymer scaffolds is desired to permit their use as therapeutics, crystal engineering materials, coatings, membranes, electronics, organo-/hydrogels, detergent formulations, personal care products, and as lubricant additives.[8,20] Controlled radical polymerization techniques have been used to prepare well-defined keto-functional polymer scaffolds for modification *via* oxime and hydrazone formation reactions.[8,18,21] The condensation product of a ketone and an alkoxyamine (*i.e.*, a ketoxime) generally possesses superior hydrolytic stability to the condensation product of an aldehyde and alkoxyamine (*i.e.*, an aldoxime). As a result, ketoxime formation has been employed for protein modification,[22] to prepare oxime functional polyketoesters,[23] and to obtain biospecific and chemoselective surface gradients.[24]

We were intrigued by the possibility of creating branched architectures containing ketoxime linkages and then capitalizing on their inherent reversibility to induce disassembly and reassembly. We reasoned that reversibility of oxime-linked macromolecules could be achieved by competitive exchange of the otherwise hydrolytically stable ketoxime in the presence of small molecule alkoxyamine or carbonyl compounds. Incorporating such stable yet exchangeable linkages in macromolecular branched architectures could lead to robust dynamic materials with potential use in encapsulating cargo (*e.g.,* drug, dyes, and fragrances), as lubricant additives, and in coating formulations.[4,19,25] As one example of a regularly branched macromolecule, well-defined star polymers are generally prepared *via* "arm-first" and "core-first" methods.[26] There is considerable interest in the preparation of star architectures that possess reversible linkages, such as alkoxyamines,[27,28] imines,[2,3,29] acylhydrazones,[30,31] boroxines,[32,33] boronic esters,[34] disulfides,[30,35,36] and Diels–Alder linkages.[37-39]

Herein, we report the synthesis of well-defined keto-functional block copolymers by RAFT polymerization and their subsequent functionalization with small molecule alkoxyamines. Addition of difunctional alkoxyamines to an aqueous solution of keto-functional block copolymers led to core-crosslinked oxime stars by an arm-first method. Due to the reversible nature of the oxime units,[6] star dissociation was induced by competitive exchange with monofunctional alkoxyamines or monofunctional aldehydes and ketones in the presence of an acid catalyst.

Results and Discussion

We reasoned that combining the high efficiency of oxime-formation with the reversibility that arises in the presence of a competitive aminooxy compound could lead to new adaptive nanoparticles and fundamental insight into the dynamic nature of oxime-containing materials. Two different ketone-containing monomers, namely 4–acryloyloxy–2–butanone (AB) and diacetone acrylamide (DAA), were polymerized by RAFT and chain extended with *N,N*–dimethylacrylamide (DMA). The resulting block copolymers were amphiphilic and contained one hydrophobic (ketone-containing) block susceptible to reaction with alkoxyamines and a second unreactive, hydrophilic block. After self-assembly into micelles in water, addition of difunctional alkoxyamines led to confined crosslinked networks that were stabilized by the passivating non-reactive blocks. These core-crosslinked stars, which can also be referred to as "core-crosslinked micelles," could be reversibly cleaved and dissociated to unimers by the addition of a monofunctional alkoxyamine that was capable of displacing the crosslinker by oxime exchange.[6] An alternative approach to dissociate the core involved the addition of a monofunctional aldehyde or ketone to effectively scavenge the crosslinker under acidic aqueous conditions.

Synthesis of block copolymers containing reactive keto-functionality *via* RAFT. Both AB and DAA were used to prepare ketone-containing block copolymers by chain extension of a poly(*N,N*–dimethylacrylamide) macro-chain-transfer-agent (PDMA macroCTA). A $PDMA_{1123}$ macroCTA was chain extended with 4–acryloyloxy 2–butanone to yield the $PDMA_{123}$–*b*–PAB_{18} (**P1**) block copolymer that contained the keto groups needed for oxime formation (Scheme 1). The number average molecular weight ($M_{n,NMR}$) of the resulting block copolymers was estimated by ^{1}H NMR spectroscopy by comparing the area of methylene protons (–OC$\underline{H}_2$–, δ = 4.2 ppm) of the pendent AB units to the area of the terminal methyl protons of the dodecyl group (–$(CH_2)_{11}$–C$\underline{H}_3$, δ = 0.85 ppm) (Table 1).

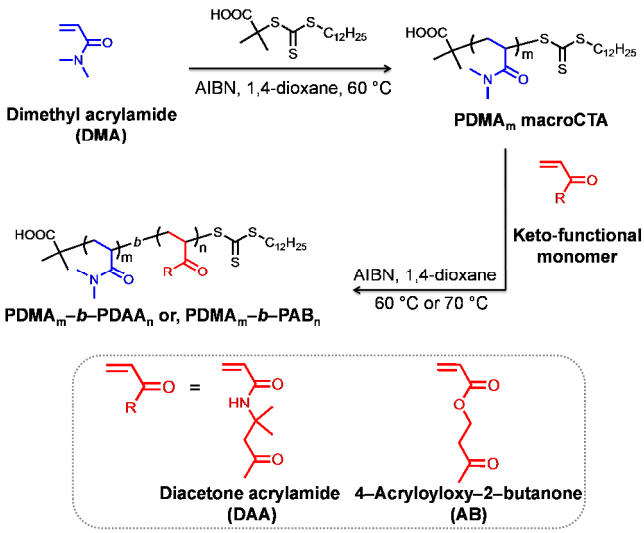

Scheme 1. Synthesis of poly(*N,N*–dimethylacrylamide) (PDMA) and its subsequent chain extension with diacetone acrylamide (DAA) and 4–acryloxy–2–butanone (AB) to prepare PDMA–*b*–PDAA and PDMA–*b*–PAB respectively.

A $PDMA_{115}$ macroCTA was also chain extended with DAA to prepare the $PDMA_{115}$–*b*–$PDAA_7$ (**P2**) block copolymer. The M_n of the block copolymers was determined by comparing the area of the methyl protons (–(C=O)–C$\underline{H}_3$, δ = 2.15 ppm) of the pendent DAA units to the terminal methyl protons of the dodecyl group (–$(CH_2)_{11}$–C$\underline{H}_3$, δ = 0.85 ppm). The discrepancy between theoretical molecular weight based on the monomer conversion ($M_{n,theo}$) and $M_{n,NMR}$ for $PDMA_{127}$–*b*–$PDAA_{14}$ (**P10**), $PDMA_{127}$–*b*–$PDAA_{39}$ (**P11**), and $PDMA_{127}$–*b*–$PDAA_{71}$ (**P12**) could be a result of the error involved in calculating the conversion, as the broad ^{1}H NMR signal of –(C=O)N$\underline{H}$– in each DAA unit (δ = 6.09 ppm) increasingly overlapped with the ^{1}H NMR signals of the vinyl peaks of DAA as the polymerization proceeded. Efficient chain extension of PDMA to yield $PDMA_{123}$–*b*–PAB_{18} (**P1**) and $PDMA_{115}$–*b*–$PDAA_7$ (**P2**) was confirmed from the clean shift of the unimodal SEC trace of the macroCTA to a lower elution time for the block copolymer (Fig. 1).

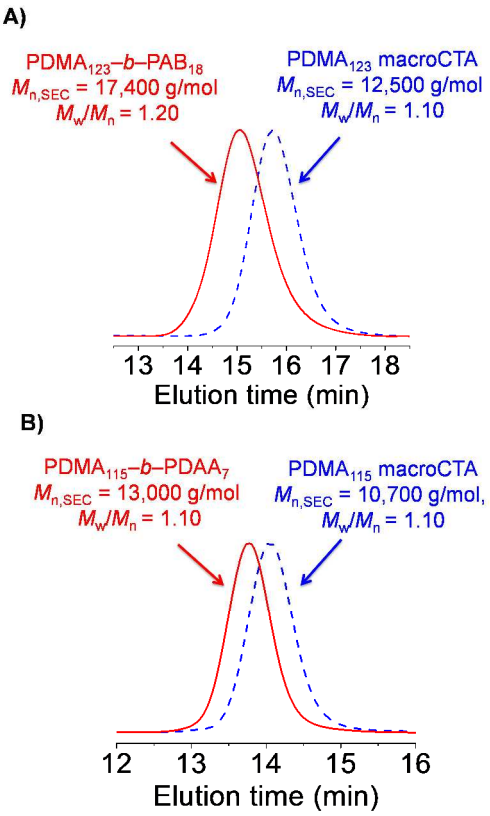

Fig. 1. Normalized refractive index traces from size exclusion chromatography of (A) poly(*N,N*–dimethylacrylamide)$_{110}$ (PDMA$_{110}$) macroCTA and PDMA$_{110}$–*b*–PAB$_{37}$ and (B) PDMA$_{115}$ macroCTA and PDMA$_{115}$–*b*–PDAA$_7$.

Functionalization of PDMA$_{110}$–*b*–PAB$_{37}$ (P3) with model alkoxyamines. While the focus of our research was to prepare adaptive nanoparticles crosslinked *via* oxime linkages, we expected keto-functional polymers could also be utilized as versatile scaffolds for post-polymerization modification. Hence, we first investigated reactions of low-molecular-weight alkoxyamines with our keto-functional block copolymers. *O*–Allyl hydroxylamine and *O*–(tetrahydro–2*H*–pyran–2–yl) hydroxylamine were chosen as model reactants for oxime-formation reaction because of the ease with which their final products could be characterized by ^{1}H NMR spectroscopy. Efficient functionalization with *O*–allyl hydroxylamine (Scheme 2) was suggested by the upfield shift of the peak corresponding to the keto methyl protons in **P3a** from 2.21 ppm to 1.85 ppm (**a** in Fig. 2A). The degree of functionalization (>95%) was calculated from the peak integral ratio for the –O–C$\underline{H_2}$–CH=CH$_2$ allylic protons and the –O–C$\underline{H_2}$–CH$_2$–C(CH$_3$)=N–O– methylene protons (Fig. 2A) in the functionalized polymer. SEC analysis (Fig. 2B) indicated a slight increase in the molecular weight of the block copolymer after the reaction (Table S1 in ESI†). Efficient functionalization (>95%) with *O*–(tetrahydro–2*H*–pyran–2–yl) hydroxylamine (Scheme 2) was also confirmed by ^{1}H NMR spectroscopy and SEC analysis (Table S1 and Fig. S2 in ESI†).

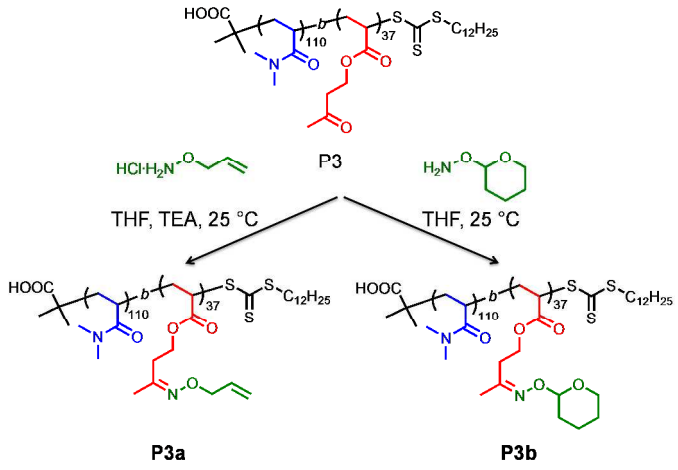

Scheme 2. Model reactions of PDMA$_{110}$–*b*–PAB$_{37}$ (**P3**) with *O*–allyl hydroxylamine and *O*–(tetrahydro–2*H*–pyran–2–yl)hydroxylamine.

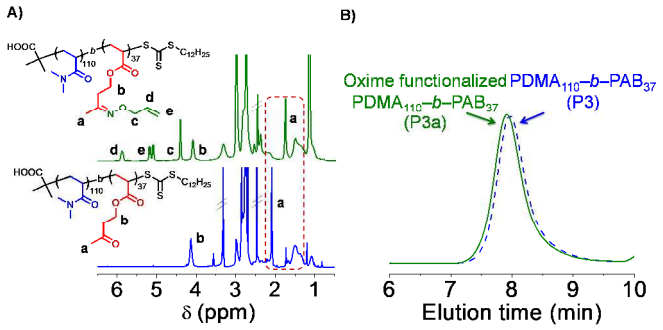

Fig. 2. Results from the model reactions of PDMA$_{110}$–*b*–PAB$_{37}$ (**P3**) with *O*–allyl hydroxylamine: (A) ^{1}H NMR spectra of PDMA$_{110}$–*b*–PDAA$_{37}$ (**P3**) before (blue) and after (green) functionalization in DMSO–d_6, (B) SEC overlay (normalized refractive index signal) of PDMA$_{110}$–*b*–PDAA$_{37}$ (**P3**) and functionalized PDMA$_{110}$–*b*–PDAA$_{37}$ (**P3a**).

Primary amines are well known to attack thiocarbonyl groups of RAFT-generated polymers to yield thiol end groups.[40] Therefore, we were curious whether the thiocarbonylthio groups at the terminus of the RAFT polymers would also be susceptible to cleavage *via* nucleophilic attack by the alkoxyamines. Such a side reaction would be expected to convert the RAFT-generated end groups to their corresponding thiols. To investigate this possibility, model reactions were conducted between PDMA$_{127}$–*b*–PDAA$_{39}$ (**P11**) and *O*–(tetrahydro–2*H*–pyran–2–yl)hydroxylamine at 25 °C at [ketone]:[alkoxyamine] ratios of 1:1 and 1:2. Interestingly, no significant reduction of the characteristic absorbance of the trithiocarbonate end group ($\lambda_{max} \approx 310$ nm) was observed after 24 h, even in the case of the excess alkoxyamine (Fig. 3A). Additionally, the SEC traces of the products from both the reactions remained monomodal after 24 h, suggesting the absence of polymer-polymer coupling *via* disulfide formation, which might be expected if significant cleavage of the trithiocarbonate moiety had occurred (Fig. 3B). The conservation of the thiocarbonylthio end-group in the presence of alkoxyamines was further confirmed by a model reaction between the original low molecular weight RAFT CTA (2–dodecylsulfanylthiocarbonylsulfanyl–2–methyl–propionic acid) and *O*–(tetrahydro–2*H*–pyran–2–yl)hydroxylamine. Similarly, no

noticeable change in the UV absorbance ($\lambda_{max} \approx 310$ nm) occurred in this case (Fig. S3, ESI†). These results suggest that end group cleavage via aminolysis by *O*–alkyl alkoxyamines is not a complicating factor.

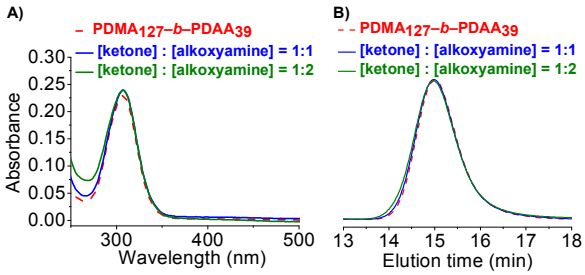

Fig. 3. (A) UV-Vis spectra of $PDMA_{127}$–*b*–$PDAA_{39}$ (**P11**) in MeOH before (control) and after its reaction with *O*–(tetrahydro–2*H*–pyran–2–yl)hydroxylamine. (B) SEC overlay (normalized refractive index signal) of $PDMA_{127}$–*b*–$PDAA_{39}$ (**P11**) before and after its reaction with *O*–(tetrahydro–2*H*–pyran–2–yl)hydroxylamine at [ketone]:[alkoxyamine] = 1:1 and 1:2.

Core-crosslinked star formation. Given the demonstrated high efficiency of oxime formation with these newly prepared keto-functional block copolymers, we turned our attention to the possibility of creating reversible core-crosslinked stars by reaction with difunctional alkoxyamines. Selective crosslinking of the reactive block of a diblock copolymer with a multifunctional crosslinker is a convenient route for the synthesis of stars.[3,27,32,34,36,38] We recently observed that pre-orientation of the block copolymers into micellar aggregates in a selective solvent prior to the crosslinking reaction drastically improves the yield and size dispersity of the resulting core-crosslinked stars.[39] PDAA demonstrates poor water solubility, making it an ideal monomer for the synthesis of amphiphilic block copolymers in which the reactive ketone is contained in the aggregated hydrophobic block.[16,41] Moreover, as compared to the acryloyl units in the AB-containing block copolymer, the acrylamido DAA units, with their adjacent gem dimethyls, are expected to have enhanced hydrolytic stability. Therefore, we decided to limit our star formation studies in aqueous media to the PDAA-containing block copolymers.

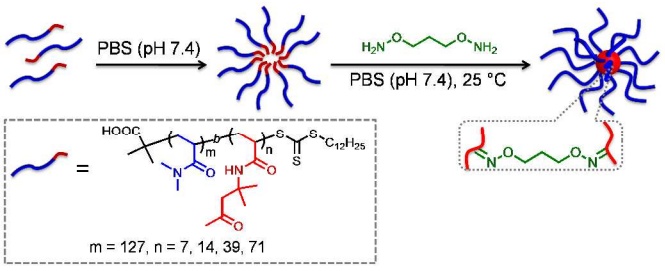

Scheme 3. Formation of core-crosslinked micelles *via* self-assembly and oxime formation.

Self-assembly of the PDMA–*b*–PDAA block copolymers was achieved by controlled dilution of a solution of the block copolymer in THF into PBS buffer (pH 7.4) (Scheme 3). SEC, light scattering, and TEM were used to characterize the resulting micelles. Depending on the length of the hydrophobic PDAA and the hydrophilic PDMA blocks, DLS measurements indicated a hydrodynamic diameter (D_h) of 17 to 36 nm for the micelles (Table 2). For example, DLS analysis of the micelles obtained from $PDMA_{127}$–*b*–$PDAA_{14}$ (**P10**, 20 mg/mL in PBS) yielded a D_h of 26 nm, while the precursor block copolymer existed as completely dissolved unimers (D_h = 6 nm) in methanol, a non-selective solvent (Fig. 4D). Addition of a difunctional alkoxyamine to the micelle solution led to crosslinking of the keto-functional hydrophobic core *via* oxime formation at 25 °C to yield core-crosslinked stars (**Star 1**). The stars were observed to have similar sizes as their original micelle precursors, as observed by DLS and TEM (Fig. 4-D, E). The covalently crosslinked nature of the stars was confirmed by their stability in methanol, a non-selective solvent that would be expected to dissociate non-crosslinked micelles to their corresponding unimers (Fig. 4D).

SEC analysis of the core-crosslinked nanostructures revealed a new peak at a lower elution volume as compared to the original unimers, indicating a significant increase in molecular weight upon assembly and crosslinking. By observing the relative deconvoluted peaks areas of the stars and unimers as a function of time, it was possible to monitor the kinetics of the crosslinking reaction (Fig. 4-A, B). In all cases, star formation was observed to be highly efficient, with typically less than 10% residual unimers being present after crosslinking. These unreacted unimers were readily removed by dialyzing the reaction solution against deionized water and isolating the purified stars by lyophilization. SEC-MALS was used to calculate the molecular weight of the resulting purified stars. The corresponding numbers of arms per star was estimated by the ratio of molecular weight of stars ($M_{w,star}$) to the molecular weight of the unimers obtained prior to crosslinking ($M_{w,arm}$) (Table 2). ^{1}H NMR spectra of the purified stars (**Star 1**) showed attenuation of the keto methyl peak [–(C=O)C$\underline{H_3}$] (2.11 ppm) and backbone protons (~1.35 ppm and 1.88 ppm) of the PDAA units, suggesting a highly crosslinked and partially desolvated core in $CDCl_3$ (Fig. S4, ESI†). We also studied star formation by selective crosslinking of the ketone-containing block of PDMA–*b*–PDAA in a non-selective solvent. *O,O'*–1,3–Propanediylbishydroxylamine was added to a solution of molecularly-dissolved $PDMA_{127}$–*b*–$PDAA_{14}$ (60 mg/mL) in methanol with [ketone]:[alkoxyamine] = 1:2 equiv. As expected, the star formation in MeOH was slower than in aqueous media (ESI†, Fig. S17). These results highlight the benefit afforded by pre-orientation of the reactive block copolymers into micelles prior to intermolecular crosslinking.

To study the star formation process in more detail, two sets of experiments were carried out to elucidate the effect of (*i*) ketone: alkoxyamine ratio, and (*ii*) the overall block copolymer concentration on the reaction kinetics and size of the resulting star nanostructures. $PDMA_{127}$–*b*–$PDAA_{14}$ was chosen for this study considering that the star formation reaction with this block copolymer was found to achieve completion within approximately 24 h, even at the lowest crosslinker equivalence used during our preliminary studies.

Journal Name RSCPublishing

ARTICLE

Table 1. Results for synthesis of block copolymers with *N,N*–dimethyl–acrylamide (DMA), 4–acryloyloxy–2–butanone (AB), and diacetone acrylamide (DAA)

Entry	Polymer	$M_{n,theo}$ [a] (kg/mol)	$M_{n,NMR}$ [b] (kg/mol)	$M_{n,SEC}$ [c] (kg/mol)	$M_{w,SEC}$ [c] (kg/mol)	M_w/M_n [c]
P1	$PDMA_{123}$–*b*–PAB_{18}	17.5	15.1	17.4	20.6	1.20
P2	$PDMA_{115}$–*b*–$PDAA_{7}$	14.1	13.5	13.0	13.7	1.10
P3	$PDMA_{110}$–*b*–PAB_{37}	17.6	16.6	15.6	19.1	1.22
P4	$PDMA_{115}$–*b*–$PDAA_{4}$	12.7	12.5	11.1	11.4	1.03
P5	$PDMA_{110}$	11.0	11.3	11.3	12.4	1.10
P6	$PDMA_{115}$	11.0	11.8	10.7	11.0	1.10
P7	$PDMA_{123}$	13.0	12.5	12.5	12.9	1.10
P8	$PDMA_{127}$	9.1	13.0	9.8	10.0	1.10
P9	$PDMA_{127}$–*b*–$PDAA_{7}$	14.4	14.2	11.0	11.0	1.10
P10	$PDMA_{127}$–*b*–$PDAA_{14}$	20.6	15.7	15.2	15.4	1.10
P11	$PDMA_{127}$–*b*–$PDAA_{39}$	28.4	19.1	19.2	19.6	1.10
P12	$PDMA_{127}$-*b*-$PDAA_{71}$	34.5	17.1	24.3	25.0	1.10

[a]Calculated from monomer conversion determined by ^{1}H NMR spectroscopy. [b]Calculated using ^{1}H NMR spectroscopy by end group analysis. [c]Determined by SEC with multiangle light scattering detection.

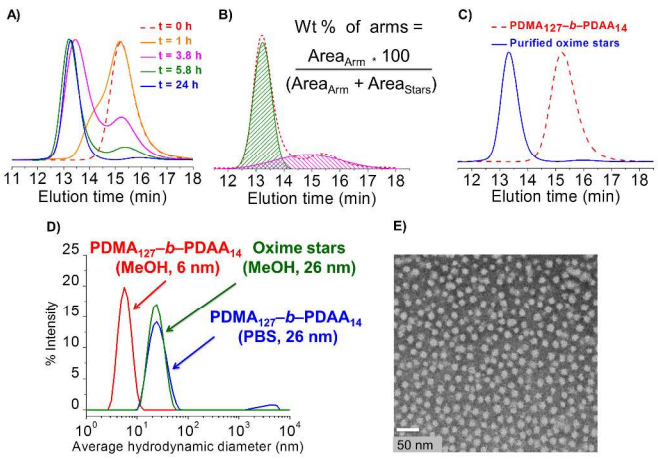

Fig. 4. (A) Normalized refractive index (RI) SEC traces showing the progress of star formation between $PDMA_{127}$–*b*–$PDAA_{14}$ (**P10,** 20 mg/mL) and *O,O'*–1,3–propanediylbishydroxylamine in PBS at [ketone]:[alkoxyamines] = 1:1 equiv. (B) Example of a deconvoluted SEC RI trace to obtain star and unimer areas. (C) Overlay of normalized SEC RI traces of $PDMA_{127}$–*b*–$PDAA_{14}$ (red) and purified oxime stars (**Star 1**, blue). (D) DLS size distribution for $PDMA_{127}$–*b*–$PDAA_{14}$ in MeOH (red), as micelles formed in PBS (blue) and as purified core-crosslinked stars in MeOH (green). (E) TEM image of purified core-crosslinked star (negative stain, scale bar: 50 nm).

First, the rate of crosslinking was studied at 25 °C in PBS with a constant polymer concentration ([$PDMA_{127}$–*b*–$PDAA_{14}$] = 20 mg/mL) using [ketone]:[alkoxyamine] equiv = 1:1, 1:2, 1:4, and 1:6). About ~53% of the micelle arms crosslinked after ~3 h with 1 equiv of difunctional alkoxyamines, whereas ~73% of micelle arms were incorporated into stars after 3 h in the presence of 2 equiv of difunctional alkoxyamines (Fig. 5A).

When the amount of difunctional alkoxyamine was further increased to 4 equiv, the conversion increased to ~81% after just 2 h and ~91% within 6 h. No significant change in the crosslinking rate was observed when the amount of difunctional alkoxyamine was further increased to 6 equiv. Almost complete conversion of micelles to stars was observed after ~25 h regardless of the amount of crosslinker used. The solution sizes (average hydrodynamic diameter, D_h) of the stars obtained after purification for all the four [ketone]:[alkoxyamine] ratios was found to be similar by both DLS (D_h = 26 nm, Table 2) and SEC (Fig. 5B).

Journal Name RSCPublishing

ARTICLE

Table 2. Molecular weight and size results of purified core-crosslinked oxime stars obtained from block copolymers of varying composition and [ketone]:[alkoxyamine] ratios

Entry	Block copolymer (star precursor)	[ketone]: [alkoxyamine] equiv	Block copolymer concentration (mg/mL)	$D_{h,micelle}$ (nm)[c]	$M_{w,star}$ (kg/mol)[a]	Arms per star ($M_{w,star}$/ $M_{w,arm}$)[b]	$D_{h,star}$ (nm)[c]
Star 1	$PDMA_{127}$–*b*–$PDAA_{14}$	1:1	20	26	660	43	26
Star 2	$PDMA_{127}$–*b*–$PDAA_{14}$	1:2	20	26	714	46	26
Star 3	$PDMA_{127}$–*b*–$PDAA_{14}$	1:4	20	26	700	45	26
Star 4	$PDMA_{127}$–*b*–$PDAA_{14}$	1:6	20	26	660	43	26
Star 5	$PDMA_{127}$–*b*–$PDAA_{7}$	1:2	10	18	192	14	19
Star 6	$PDMA_{127}$–*b*–$PDAA_{7}$	1:2	20	18	205	14	19
Star 7	$PDMA_{127}$–*b*–$PDAA_{14}$	1:2	10	25	700	45	25
Star 8	$PDMA_{127}$–*b*–$PDAA_{39}$	1:2	10	30	1600	81	32
Star 9	$PDMA_{127}$–*b*–$PDAA_{39}$	1:2	20	34	1620	83	31
Star 10	$PDMA_{127}$–*b*–$PDAA_{71}$	1:2	10	34	2510	101	36
Star 11	$PDMA_{127}$–*b*–$PDAA_{71}$	1:2	20	35	2550	102	37
Star 12	$PDMA_{115}$–*b*–$PDAA_{7}$	1:2	20	19	340	26	24

[a]**Weight-average** molecular weight of the stars determined by SEC using multiangle light scattering (MALS). [b]**Weight-average** number of arms per star determined by dividing $M_{w,star}$ by $M_{w,arm}$. [c]**Hydrodynamic diameter** determined by dynamic light scattering (DLS) in methanol.

The M_w of the stars ranged between 660–700 kg/mol corresponding to 43–46 arms per star. These findings indicate that while increasing the amount of crosslinker increases the rate of core crosslinking, completely crosslinked cores are obtained even at [ketone]:[alkoxyamine] = 1:1 equiv.

The efficiency and kinetics of star formation was also investigated as a function of block copolymer composition and concentration. Micellization and star-formation was studied for several block copolymers having the same length of the passive $PDMA_{127}$ block and different lengths of the reactive PDAA block at a [ketone]: [alkoxyamine] ratio of 1:2 equiv (Fig. 6). For the block copolymers with a degree of polymerization of the PDAA block between 14 to 71 units, the initial rate and the final extent of star formation increased slightly with increasing polymer concentration from 10 to 20 mg/mL (Fig. 6A and 6B). However, a larger increase in initial reaction rate and final extent of star formation was observed for the block copolymer with the shortest PDAA segment ($PDMA_{127}$–*b*–$PDAA_{7}$) on increasing the polymer concentration from 10 to 20 mg/mL. For example, at 10 mg/mL only 22% of the block copolymer arms were incorporated into the stars in ~ 27 h, whereas at 20 mg/mL the conversion of arms to stars was 65% in the same time.

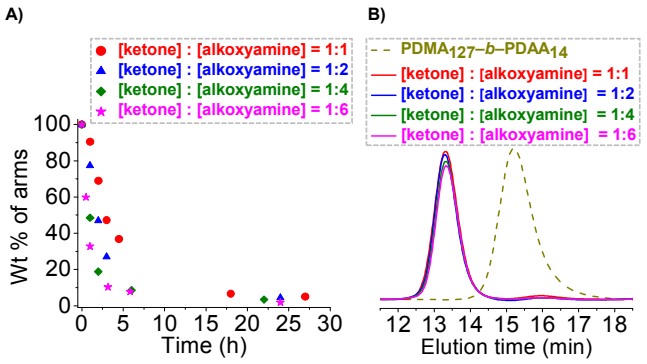

Fig. 5. (A) Kinetics of star formation (**Star 1**–**4**, Table 2) determined by deconvolution of the normalized SEC refractive index traces obtained during the reaction between $PDMA_{127}$–*b*–$PDAA_{14}$ (**P10**) and *O,O'*–1,3–propanediylbishydroxylamine dihydrochloride at varying [ketone]:[alkoxyamine] ratios. (B) Normalized SEC refractive index traces of $PDMA_{127}$–*b*–$PDAA_{14}$ and the resulting purified stars (**Star 1**–**4**, Table 2).

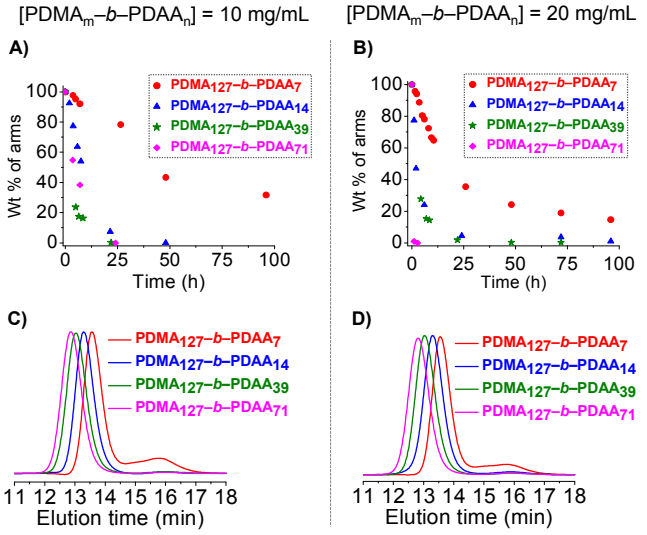

Fig. 6. Kinetics of star formation for PDMA–*b*–PDAA block copolymers determined by deconvolution of SEC refractive index traces at a block copolymer concentration of (A) 10 mg/mL and (B) 20 mg/mL. SEC (normalized refractive index) traces of purified stars obtained from PDMA–*b*–PDAA block copolymers at concentrations of (C) 10 mg/mL and (D) 20 mg/mL.

While the final conversion to stars was almost quantitative in the case of the block copolymers with degrees of polymerization for the PDAA block between 14 to 71, only 86% conversion was observed for $PDMA_{127}$–*b*–$PDAA_7$, even after 96 h ([$PDMA_{127}$–*b*–$PDAA_7$] = 20 mg/mL). The solution size and molecular weight of the stars were also found to increase with increasing length of the reactive PDAA block length (Table 2). Interestingly, no change in D_h and M_w was observed with increasing polymer concentration. It should be noted that in all cases the solution sizes of the stars were almost the same as those of the non-crosslinked micelles from which they were prepared. These observations indicate that the average number of arms for stars obtained by crosslinking of pre-organized micelles is dictated primarily by the equilibrium size of the micelles and likely not by the concentration of polymer and crosslinker. Thus, the morphology of the self-assembled aggregates of the reactive block copolymers is likely preserved after crosslinking, and various reversibly crosslinked nano-/micro-aggregates like micelles, vesicles, rods *etc*., can possibly be obtained by using this protocol of self-assembly followed by a covalent crosslinking process. The results also indicate that a fine balance between the number of reactive functional groups in the block copolymer and polymer concentration leads to higher efficiency of the crosslinking reaction. Certainly, a higher number of reactive groups per polymer chain leads to more efficient crosslinking, as it ensures the presence of a sufficient number of functional groups for intermolecular crosslinking despite unavoidable intramolecular reactions. The concentration of block copolymers and the stoichiometry employed in this study were sufficient to achieve near-quantitative conversion of the micelles to stars in most cases.

Disassembly of core-crosslinked oxime stars *via* oxime exchange. While the enhanced stability and controlled exchange of oxime linkages has been utilized in analytical chemistry for isolation of small molecules,[42] synthesis of polymer scaffolds, and main chain oxime-linked amphiphilic copolymers,[43] reversible assembly of oxime-containing polymers has remained largely unexplored.

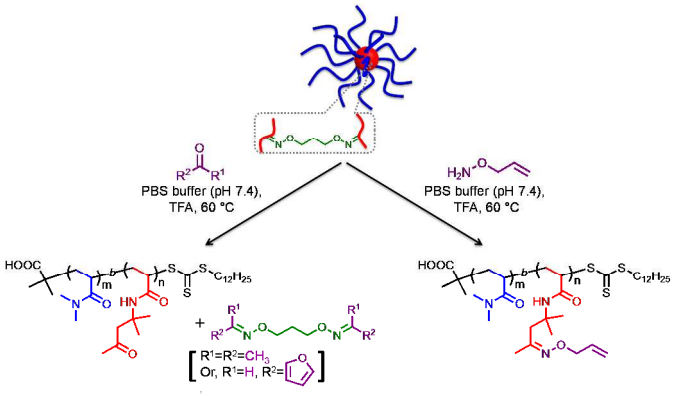

Scheme 4. Disassembly of core-crosslinked oxime stars by competitive exchange with monofunctional aldehydes/ketones or monofunctional alkoxyamines.

Oxime bonds provide the opportunity for reversible disassembly *via* competitive oxime exchange under acidic conditions.[6,44] We reasoned that star dissociation could be triggered in the presence of added monofunctional alkoxyamines or monofunctional aldehydes/ketones that compete for binding with the polymer or difunctional alkoxyamine crosslinker (Scheme 4). To investigate this possibility, a solution of purified stars was treated with furfuraldehyde in the presence of trifluroacetic acid (TFA) at 60 ºC. The pH of the reaction solution was found to be ~4 after addition of TFA. Under these conditions, approximately 82 and 100% disassociation of the stars was observed after 10.5 h and 24 h, respectively (Fig. 7A and B). DLS confirmed complete dissociation of the stars (D_h = 24 nm) to individual $PDMA_{115}$–*b*–$PDAA_7$ chains (D_h = 5 nm) (Fig. 7C). Stars could also be dissociated *via* competitive exchange in the presence of monofunctional alkoxyamines under similar experimental conditions (Fig. S16, ESI†).

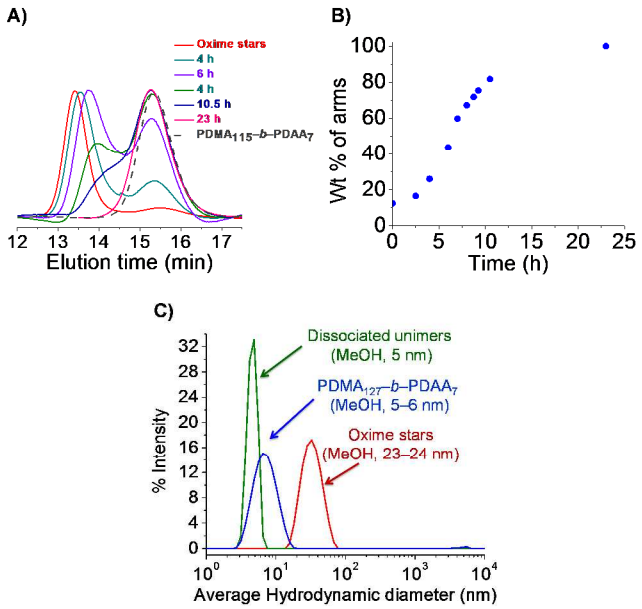

Fig. 7 (A) Overlay of SEC refractive index traces. (B) Kinetics of star dissociation determined by deconvolution of the SEC refractive index traces during the reaction between a core-crosslinked oxime star (**Star 12**) and furfuraldehyde in presence of TFA at 60 °C. (C) DLS size distribution of oxime stars (red), unimers (blue), and unimers after star dissociation (green).

Conclusions

Oxime formation between ketone-containing block copolymers and difunctional alkoxyamines is clearly a viable means to prepare core-crosslinked stars. A variety of factors control the efficiency of star formation, including solvent quality (*i.e.*, selective *vs*. non-selective), stoichiometry, and block copolymer composition/concentration. An increase in the rate of core-crosslinking was observed with increasing block copolymer concentration. The star formation kinetics at a constant block copolymer concentration and stoichiometry was also found to be accelerated when the reactive ketone-containing block length was varied from 7 to 71. These results clearly demonstrate the efficiency of oxime formation is convenient for the facile preparation of core-crosslinked star polymers.

The susceptibility of the stars to disassembly suggests oximes are useful linkages to employ in the construction of dynamic-covalent materials. The reversible nature of oxime linkages in the crosslinked core made it possible to disassemble the stars under conditions that promote oxime exchange in the presence of small alkoxyamine or carbonyl compounds. To our knowledge, the reversible nature of oxime-containing polymeric architectures has not been previously explored. The tuneable reversibility of the oxime equilibrium can potentially be utilized for transporting and releasing cargo of fragrances, dyes, and drugs. Moreover, even though the work described here relies on assemblies in solution, application of oxime chemistry could be extended to rehealable gels and bulk materials by careful selection of reagents and controlling branching properties.

Acknowledgement

This material is based upon work supported by the National Science Foundation (DMR-1410223).

Notes and References

George & Josephine Butler Polymer Research Laboratory, Center for Macromolecular Science & Engineering, Department of Chemistry, University of Florida, Gainesville, FL 32611-7200, USA
E-Mail: sumerlin@chem.ufl.edu

†Electronic Supplementary Information (ESI) available NMR, SEC traces, TEM images of oxime functional star. See DOI: 10.1039/x0xx00000x

1. G. Deng, F. Li, H. Yu, F. Liu, C. Liu, W. Sun, H. Jiang and Y. Chen, *ACS Macro Lett.*, 2012, **1**, 275-279; X. Wang, L. Wang, S. Yang, M. Zhang, Q. Xiong, H. Zhao and L. Liu, *Macromolecules*, 2014, **47**, 1999-2009; A. Herrmann, *Org. Biomol. Chem.*, 2009, **7**, 3195-3204; T. C. Lai, H. Cho and G. S. Kwon, *Polym. Chem.*, 2014, **5**, 1650-1661; Y. Zhang, C. Xiao, M. Li, J. Ding, C. He, X. Zhuang and X. Chen, *Polym. Chem.*, 2014, **5**, 2801-2808; W. G. Skene and J.-M. P. Lehn, *PNAS*, 2004, **101**, 8270-8275.
2. A. W. Jackson and D. A. Fulton, *Chem. Commun.*, 2011, **47**, 6807-6809.
3. A. W. Jackson, C. Stakes and D. A. Fulton, *Polym. Chem.*, 2011, **2**, 2500-2511.
4. J.-M. Lehn, *Prog. Polym. Sci.*, 2005, **30**, 814-831.
5. J. Kalia and R. T. Raines, *Angew. Chem. Int. Ed.*, 2008, **47**, 7523-7526.
6. V. A. Polyakov, M. I. Nelen, N. Nazarpack-Kandlousy, A. D. Ryabov and A. V. Eliseev, *J. Phys. Org. Chem.*, 1999, **12**, 357-363.
7. A. Pulsipher, D. Dutta, W. Luo and M. N. Yousaf, *Angew. Chem. Int. Ed.*, 2014, DOI: 10.1002/anie.201404099; S. Park, N. P. Westcott, W. Luo, D. Dutta and M. N. Yousaf, *Bioconjugate Chem.*, 2014, **25**, 543-551.
8. J. Liu, R. C. Li, G. J. Sand, V. Bulmus, T. P. Davis and H. D. Maynard, *Macromolecules*, 2012, **46**, 8-14.
9. K. J. Mackenzie and M. B. Francis, *J. Am. Chem. Soc.*, 2012, **135**, 293-300.
10. A. P. Esser-Kahn, V. Trang and M. B. Francis, *J. Am. Chem. Soc.*, 2010, **132**, 13264-13269.
11. A. P. Esser-Kahn and M. B. Francis, *Angew. Chem. Int. Ed.*, 2008, **47**, 3751-3754.
12. K. L. Christman, R. M. Broyer, Z. P. Tolstyka and H. D. Maynard, *J. Mater. Chem.*, 2007, **17**, 2021-2027.
13. Z. P. Tolstyka, W. Richardson, E. Bat, C. J. Stevens, D. P. Parra, J. K. Dozier, M. D. Distefano, B. Dunn and H. D. Maynard, *ChemBioChem*, 2013, **14**, 2464-2471.
14. M. R. Hill, S. Mukherjee, P. J. Costanzo and B. S. Sumerlin, *Polym. Chem.*, 2012, **3**, 1758-1762.
15. N. Metz and P. Theato, *Eur. Polym. J.*, 2007, **43**, 1202-1209.
16. X. Tang, J. Han, Z. Zhu, X. Lu, H. Chen and Y. Cai, *Polym. Chem.*, 2014, DOI: 10.1039/c4py00146j.
17. A. W. Jackson and D. A. Fulton, *Polym. Chem.*, 2013, **4**, 31-45; J. Hwang, R. C. Li and H. D. Maynard, *J. Controlled Release*, 2007, **122**, 279-286; K. A. Günay, P. Theato and H.-A. Klok, *Functional Polymers by Post-Polymerization Modification: Concepts, Guidelines, and Applications*, Wiley-VCH Verlag GmbH & Co. KGaA, 2012, pp. 1-44.

18. S. Bandyopadhyay, X. Xia, A. Maiseiyeu, G. Mihai, S. Rajagopalan and D. Bong, *Macromolecules*, 2012, **45**, 6766-6773.
19. P. T. Corbett, J. Leclaire, L. Vial, K. R. West, J.-L. Wietor, J. K. M. Sanders and S. Otto, *Chem. Rev.*, 2006, **106**, 3652-3711.
20. K. Matyjaszewski and J. Spanswick, *Mater. Today*, 2005, **8**, 26-33.
21. C. Cheng, G. Sun, E. Khoshdel and K. L. Wooley, *J. Am. Chem. Soc.*, 2007, **129**, 10086-10087; T. Krasia, R. Soula, H. G. Borner and H. Schlaad, *Chem. Commun.*, 2003, 538-539.
22. R. E. Kieltyka, M. M. C. Bastings, G. C. van Almen, P. Besenius, E. W. L. Kemps and P. Y. W. Dankers, *Chem. Commun.*, 2012, **48**, 1452-1454; Y.-X. Chen, G. Triola and H. Waldmann, *Acc. Chem. Res.*, 2011, **44**, 762-773; L. Yi, Y.-X. Chen, P.-C. Lin, H. Schroder, C. M. Niemeyer, Y.-W. Wu, R. S. Goody, G. Triola and H. Waldmann, *Chem. Commun.*, 2012, **48**, 10829-10831; V. Vázquez-Dorbatt, Z. P. Tolstyka and H. D. Maynard, *Macromolecules*, 2009, **42**, 7650-7656.
23. D. G. Barrett and M. N. Yousaf, *Biomacromolecules*, 2008, **9**, 2029-2035.
24. B. M. Lamb, S. Park and M. N. Yousaf, *Langmuir*, 2010, **26**, 12817-12823.
25. S. J. Rowan, S. J. Cantrill, G. R. L. Cousins, J. K. M. Sanders and J. F. Stoddart, *Angew. Chem. Int. Ed.*, 2002, **41**, 898-952; R. J. Wojtecki, M. A. Meador and S. J. Rowan, *Nat. Mater.*, 2011, **10**, 14-27.
26. J. Ding and S. Holdcroft, *Aust. J. Chem.*, 2012, **65**, 1117-1123; H. Gao and K. Matyjaszewski, *J. Am. Chem. Soc.*, 2007, **129**, 11828-11834; H. Shohi, M. Sawamoto and T. Higashimura, *Macromolecules*, 1991, **24**, 4926-4931; C. Zhang, M. Miao, X. Cao and Z. An, *Polym. Chem.*, 2012, **3**, 2656-2664; X. Cao, C. Zhang, S. Wu and Z. An, *Polym. Chem.*, 2014, **5**, 4277-4284; J. Liu, H. Duong, M. R. Whittaker, T. P. Davis and C. Boyer, *Macromol. Rapid Commun.*, 2012, **33**, 760-766.
27. Y. Amamoto, Y. Higaki, Y. Matsuda, H. Otsuka and A. Takahara, *J. Am. Chem. Soc.*, 2007, **129**, 13298-13304.
28. Y. Amamoto, M. Kikuchi, H. Masunaga, S. Sasaki, H. Otsuka and A. Takahara, *Macromolecules*, 2010, **43**, 1785-1791; Y. Amamoto, M. Kikuchi, H. Otsuka and A. Takahara, *Polym. J.*, 2010, **42**, 860-867.
29. A. W. Jackson and D. A. Fulton, *Chem. Commun.*, 2010, **46**, 6051-6053; X. Cai, C. Dong, H. Dong, G. Wang, G. M. Pauletti, X. Pan, H. Wen, I. Mehl, Y. Li and D. Shi, *Biomacromolecules*, 2012, **13**, 1024-1034; Z.-M. Wu, H. Liang, J. Lu and W.-L. Deng, *J. Polym. Sci., Part A: Polym. Chem.*, 2010, **48**, 3323-3330.
30. Q. Wang, L. Zhu, G. Li, C. Tu, Y. Pang, C. Jin, B. Zhu, X. Zhu and Y. Liu, *Macromol. Biosci.*, 2011, **11**, 1553-1562.
31. L. Zhu, Y. Shi, C. Tu, R. Wang, Y. Pang, F. Qiu, X. Zhu, D. Yan, L. He, C. Jin and B. Zhu, *Langmuir*, 2010, **26**, 8875-8881.
32. P. De, S. R. Gondi, D. Roy and B. S. Sumerlin, *Macromolecules*, 2009, **42**, 5614-5621.
33. Y. Qin, C. Cui and F. Jäkle, *Macromolecules*, 2007, **40**, 1413-1420.
34. A. P. Bapat, D. Roy, J. G. Ray, D. A. Savin and B. S. Sumerlin, *J. Am. Chem. Soc.*, 2011, **133**, 19832-19838.
35. A. Sulistio, A. Blencowe, A. Widjaya, X. Zhang and G. Qiao, *Polym. Chem.*, 2012, **3**, 224-234; J. Kamada, K. Koynov, C. Corten, A. Juhari, J. A. Yoon, M. W. Urban, A. C. Balazs and K. Matyjaszewski, *Macromolecules*, 2010, **43**, 4133-4139; H. Gao, N. V. Tsarevsky and K. Matyjaszewski, *Macromolecules*, 2005, **38**, 5995-6004.
36. A. P. Bapat, J. G. Ray, D. A. Savin and B. S. Sumerlin, *Macromolecules*, 2013, **46**, 2188-2198.
37. N. Aumsuwan and M. W. Urban, *Polymer*, 2009, **50**, 33-36.
38. J. A. Syrett, G. Mantovani, W. R. S. Barton, D. Price and D. M. Haddleton, *Polym. Chem.*, 2010, **1**, 102-106.
39. A. P. Bapat, J. G. Ray, D. A. Savin, E. A. Hoff, D. L. Patton and B. S. Sumerlin, *Polym. Chem.*, 2012, **3**, 3112-3120.
40. A. B. Lowe, *Polym. Chem.*, 2014, **5**, 4820-4870; J. Vandenbergh and T. Junkers, *Polym. Chem.*, 2012, **3**, 2739-2742; M. D. Rowe, C.-C. Chang, D. H. Thamm, S. L. Kraft, J. F. Harmon, A. P. Vogt, B. S. Sumerlin and S. G. Boyes, *Langmuir*, 2009, **25**, 9487-9499; H. Willcock and R. K. O'Reilly, *Polym. Chem.*, 2010, **1**, 149-157; F. S. H. Krismastuti, W. L. A. Brooks, M. J. Sweetman, B. S. Sumerlin and N. H. Voelcker, *J. Mater. Chem. B*, 2014, **2**, 3972-3983.
41. M. Schilli Christine, H. E. Müller Axel, E. Rizzardo, H. Thang San and Y. K. Chong, *Advances in Controlled/Living Radical Polymerization*, American Chemical Society, 2003, pp. 603-618.
42. M. Axelson, *Anal. Biochem.*, 1978, **86**, 133-141.
43. M. Rashidian, M. M. Mahmoodi, R. Shah, J. K. Dozier, C. R. Wagner and M. D. Distefano, *Bioconjugate Chem.*, 2013, **24**, 333-342; Y. Jin, L. Song, Y. Su, L. Zhu, Y. Pang, F. Qiu, G. Tong, D. Yan, B. Zhu and X. Zhu, *Biomacromolecules*, 2011, **12**, 3460-3468.
44. R. Kaiser, *Perfumes*, eds. P. M. Müller and D. Lamparsky, Springer Netherlands, 1994, pp. 213-250.